A NUMERICAL SIMULATION OF ONE-DIMENSIONAL DOPANT DIFFUSION IN OXIDISING SILICON

R.O. MOODY and C.P. PLEASE[†]

Numerical Analysis Report 3/87

Department of Mathematics, University of Reading.

[†] Present address: Department of Mathematics, University of Southampton.

CONTENTS

ABSTRACT

This paper presents details of a one-dimensional numerical simulation of the redistribution of dopant concentrations during the thermal oxidation of silicon. The mathematical model is governed by a non-linear partial differential equation, and contains a moving interface whose motion is prescribed and at which there are coupled silicon and oxide dopant concentration conditions.

A non-dimensionalisation of the original problem reveals insignificant diffusion in the oxide region, enabling a partial decoupling of the silicon and oxide dopant concentration sub-problems. A transformation of the concentration variable in the silicon region is made, the moving finite element method is applied to the modified differential equations, and the resulting system is solved using an iterative technique. The dopant concentration profile in the oxide is then determined by applying an advection argument to the known interface silicon dopant concentrations.

1. INTRODUCTION

Silicon oxide is grown in metal oxide semiconductor field effect transistors (MOSFET's) in order to electrically isolate one such device from its direct neighbours and to provide insulated surfaces for device interconnections. Before thermal oxide growth commences, high concentration dopant (in the form of boron, phosphorus, arsenic or a combination of these) is implanted into crystalline silicon, and this serves to provide source/drain regions and to further increase electrical isolation between devices. The dopant then diffuses in the diminishing silicon and enlarging oxide regions. The thermal oxidation of silicon comprises two distinct physical processes: firstly the diffusion of the oxygen through the oxide to the silicon-oxide interface (where the oxide forms, causing stresses which result in motion) and secondly, the diffusion of the dopant in the silicon and oxide regions. These two processes, however, can be decoupled if it is assumed that the oxidation rate is independent of the dopant concentration.

The interface motion and dopant diffusion problems have been studied by many workers in both one and two dimensions. Experimental work on a one-dimensional form of the first problem by Deal and Grove [1] has indicated the existence of a temperature-dependent linear-parabolic oxide growth rate law, which Massoud et al. [2] have implemented to determine accurate values for its rate constants. King [3] has considered an analytic solution of the two-dimensional interface motion problem. A numerical finite element solution of this problem has been produced by Stettler et al. [4], and Chorin's pressure-velocity algorithm [5] has been implemented in [6],[7] with boundary techniques, and in [8] with the finite element method.

The dopant diffusion problem has been solved numerically, both on fixed silicon domains (in [9],[10] in one dimension and [11] in two), and also on those which include a moving oxide boundary. Efforts of the latter type can be divided into two categories : those which do not solve for the dopant concentrations in the growing oxide region, and those which do. Authors of the first category include Budil et al. [12], in one dimension, and Penumalli [13], Maldonado et al. [14], Taniguchi et al. [15] and Desoutter et al. [16], in two. The finite difference approaches of [13] and [14] include the transformation of the time-dependent silicon domain onto one which is stationary in time. The physical domain is considered in [15] and [16], where finite difference and element techniques, respectively, are employed. Koltai and Trutz [17] include continuous grid deformation in their numerical method for determining dopant concentration profiles in both the silicon and oxide regions. This problem has also been studied by Borucki et al. [18], whose finite element technique is implemented together with an automatic mesh generator in the two regions.

In this paper we consider a one-dimensional model of the dopant diffusion moving boundary problem. Our code contains the user-specification of both clustering (see [10]) and oxidation. In the silicon we obtain a numerical solution in the physical domain using the moving finite element (MFE) method ([19],[20],[21]), which is attractive due to its ability to accurately track moving boundaries. Oxide dopant concentration profiles are also displayed, using the known silicon information.

In section 2 we present the mathematical model and discuss its main features, leading to an important simplification. The solution technique

for the simplified problem is described in detail in section 3. Section 4 contains the numerical results, which are then analysed in 5 where conclusions are also drawn.

2. THE MATHEMATICAL MODEL

The one-dimensional model considered here is that of Fair [22], which contains only one diffusing species.

2.1 Diffusion Equations and Accompanying Conditions

We shall assume that the silicon is stationary and that the oxide motion obeys the Deal and Grove rule ([1]). Let

$$s(t) = \tfrac{1}{2} \{ \sqrt{A^2 + 4[s(0)^2 + As(0) + Bt]} - A \} \quad , \tag{2.1}$$

(where B and B/A are the respective parabolic and linear temperature-dependent rate constants) denote the position of the silicon-oxide interface at time t. Then, owing to the expansion which occurs when silicon oxidises to silicon dioxide, the external oxide boundary moves with a velocity

$$-(\gamma-1)\,\dot{s}(t) \quad ,$$

where the dot denotes differentiation with respect to time and γ is the silicon-oxide specific volumes ratio. The silicon and oxide regions are taken to be

$$(s(t), s_r) \quad \text{and} \quad (s_l(t), s(t)) \quad ,$$

respectively, where s_r is constant and

$$s_l(t) = s_l(0) - (\gamma-1)\,[s(t) - s(0)]. \tag{2.2}$$

The partial differential equation governing dopant diffusion in the silicon is

$$\frac{\partial c_s}{\partial t} = \frac{\partial}{\partial x} \left\{ D_s(c_s) \frac{\partial c_s}{\partial x} \right\} \quad . \tag{2.3}$$

Here c_s denotes the total dopant concentration (which can be expressed as the sum of its active, c_s^A, and clustered, c_s^C parts), and

$$D_s(c_s) = D_i \left\{ \frac{1 + \beta[n_e(c_s)/n_i]}{1 + \beta} \right\} , \tag{2.4}$$

where D_i, β and n_i are constant. The local electrical charge is

$$n_e(c_s) = \tfrac{1}{2} \left\{ \left[\frac{\alpha}{\alpha+1} c_s^A + \frac{1}{\alpha+1} c_s^C \right] + \sqrt{\left[\frac{\alpha}{\alpha+1} c_s^A + \frac{1}{\alpha+1} c_s^C \right]^2 + 4n_i^2} \right\} \tag{2.5}$$

where α is the ratio of the electric charge of an active atom to that of a clustered one ([10]). The diffusion of dopant in silicon dioxide, which must account for oxide motion, obeys the equation

$$\frac{\partial c_o}{\partial t} = D_o \frac{\partial^2 c_o}{\partial x^2} + (\gamma-1)\, \dot{s}(t) \frac{\partial c_o}{\partial x} , \tag{2.6}$$

where c_o is the total dopant concentration and D_o the diffusion coefficient. In keeping with previous workers, we do not account for clustering effects in the oxide.

We shall consider homogeneous Neumann conditions, namely,

$$D_s(c_s) \frac{\partial c_s}{\partial x} = 0 , \quad x = s_r , \tag{2.7)(a}$$

$$D_o \frac{\partial c_o}{\partial x} = 0 , \quad x = s_l(t) \tag{2.7)(b}$$

which model no flux leakage at external boundaries.

We assume that the dopant flux across the moving interface is continuous. This flux is determined by a simple chemical reaction which attempts to segregate the interface silicon and oxide dopant concentrations in a particular ratio. The resulting conditions are:

$$D_s(c_s)\,\frac{\partial c_s}{\partial x} + \dot{s}(t)c_s = -h\,(c_o - c_s/m) \quad , \tag{2.8)(a}$$

$$D_o\,\frac{\partial c_o}{\partial x} + \gamma\,\dot{s}(t)\,c_o = -h\,(c_o - c_s/m) \quad , \tag{2.8)(b}$$

where h and m are respectively the boundary transport rate and equilibrium segregation ratio. Similar conditions appear in [8] and [18] - but without the important advective terms!

Ion implantation into silicon typically produces a Gaussian dopant profile. Our initial data in this region is therefore taken to be

$$c_s(x,0) = \frac{N}{\sigma\sqrt{2\pi}}\,\exp\,[\,-(x-R)^2 / 4\sigma^2\,] \quad , \tag{2.9)(a}$$

where N, σ and R are respectively the dose, straggle and depth of the Gaussian. If oxide is present at the outset, then we assume the layer to be sufficiently thin that its dopant concentration is initially constant, yielding the condition:

$$c_o(x,0) = c_s(s(0),0) \quad . \tag{2.9)(b}$$

2.2 Simplification of the Original Model

In order to determine the most important features of our problem, we non-dimensionalise as follows:

$$\left.\begin{aligned} c_s &= n_i \; C_s \\ c_o &= n_i \; C_o \\ x &= L \; X \\ t &= \frac{L^2}{D_i} \; T \\ s(t) &= s(0) + S_o \; S(T) \\ D_s(c_s) &= D_i \; D_S \; (C_s) \end{aligned}\right\} , \tag{2.10}$$

where upper case symbols denote the non-dimensional form of the corresponding physical variables. Here the constants n_i , L , D_i and S_o are representative of the dopant concentration, initial thickness of silicon, diffusion coefficient and depth to be oxidised in the silicon region.

The diffusion equations (2.3) and (2.6) respectively become

$$\frac{\partial C_s}{\partial T} = \frac{\partial}{\partial X} \left\{ D_S(C_s) \; \frac{\partial C_s}{\partial X} \right\} , \tag{2.11}$$

and

$$\frac{\partial C_o}{\partial T} = \delta_1 \frac{\partial^2 C_o}{\partial X^2} + \delta_2 \, (\gamma - 1) \; S'(T) \; \frac{\partial C_o}{\partial X} , \tag{2.12}$$

where the dash denotes differentiation with respect to the dimensionless time variable, and δ_1, δ_2 are constants. The external boundary conditions

If we, therefore, neglect diffusion in (2.12), then the p.d.e. becomes

$$\frac{\partial C_o}{\partial T} = \delta_2(\gamma-1)\, S'(T)\, \frac{\partial C_o}{\partial X} \quad , \tag{2.17}$$

which is of first order and so does not require the external boundary condition (2.13)(b). The additional assumption of equilibrium segregation at the interface allows a modification of conditions (2.14):

$$\frac{1}{\delta_2} D_S(C_s) \frac{\partial C_s}{\partial X} + S'(T)\, C_s = \gamma S'(T) C_o \tag{2.18)(a}$$

$$C_o - C_s/m = 0 \quad . \tag{2.18)(b}$$

Substitution of the oxide dopant concentration from (2.18)(b) into (2.18)(a) results in

$$\frac{1}{\delta_2} D_S(C_s) \frac{\partial C_s}{\partial X} + S'(T)\,[1-\gamma/m]\, C_s = 0 \quad , \tag{2.19)(a}$$

$$C_o = C_s/m \quad . \tag{2.19)(b}$$

We note that these are inconsistent with the initial data, and this point will be discussed in detail in section 3.1.4.

The non-dimensionalisation analysis has therefore enabled us to almost completely decouple the silicon and oxide dopant diffusion sub-problems. Hence, our solution approach is to first solve the silicon sub-problem, and then use this information to obtain an oxide dopant concentration profile.

3. METHOD OF SOLUTION

In this section we describe the numerical techniques employed to determine dopant concentration profiles in the silicon region, and also, how corresponding oxide ones are obtained using this information.

3.1 Numerical Solutuion of the Silicon Sub-problem

We now describe the numerical solution technique used for the simplified problem in the silicon region. The method contains prescriptions for the following difficulties encountered: the presence of steep fronts, initial node placement, inconsistent initial data and implementation of the interface condition (2.19)(a).

3.1.1 The Moving Finite Element Method

Here we briefly describe the one-dimensional form of the MFE method, which was introduced by Miller and Miller [19], and further analysed by Miller [20] and Wathen and Baines [21]. We consider the case of piecewise linear basis functions and so seek an approximate solution which is continuous and consists of straight line segments ([19],[20],[21]).

Differentiation of the assumed form of the solution with respect to time produces an expression involving nodal value and position velocities ([19],[20],[21]). Now the second order differential operator terms in the p.d.e. act on the piecewise linear form of solution to produce a series of delta functions. To overcome this problem we employ a recovery technique and this yields smoother estimates of the troublesome derivative terms ([23]). The square of the L_2 norm of the residual of the differential equation is minimised over these unknown velocities, and this produces a 2x2 block tridiagonal

system of linear equations. A diagonal block pre-conditioned conjugate gradient method ([24]) may then be used to efficiently invert this system ([25]) to yield a velocity vector. The nodal positions and values are then updated by applying the first order Euler time-stepping scheme to this vector ([21]), with the time increment being chosen to prevent nodes from colliding ([21]) and preserve accuracy of the numerical solution (for details, see section 3.1.5).

3.1.2 Resolution of Steep Fronts

The presence of propagating steep fronts in the silicon causes severe numerical difficulties. Please and Sweby [26] have overcome such problems by transforming the dependent variable into one which represents a velocity potential. In the present case, the new variable, Φ_s, is given by

$$\Phi_s = C_s/n_i + \ln \{C_s / n_i\} \ . \tag{3.1}$$

This transformation causes the partial differential equation (2.11) and conditions (2.13)(a), (2.19)(a) and (2.15)(a) to respectively become

$$\frac{\partial \Phi_s}{\partial T} = \frac{C_s+1}{C_s} \frac{\partial}{\partial X} \left\{ \frac{C_s D_S(C_s)}{C_s+1} \frac{\partial \Phi_s}{\partial X} \right\} , \tag{3.2}$$

$$\frac{C_s D_S(C_s)}{C_s+1} \frac{\partial \Phi_s}{\partial X} = 0 , \tag{3.3}$$

$$\frac{1}{\delta_2} \frac{C_s D_S(C_s)}{C_s+1} \frac{\partial \Phi_s}{\partial X} + S'(T) [1-\gamma/m] C_s = 0 , \tag{3.4}$$

$$\Phi_s(X,0) = C_s(X,0) + \ln \{ C_s(X,0) \} , \tag{3.5}$$

which constitute the dopant diffusion problem in the silicon region.

3.1.3 Initial Node Placement

As previously mentioned, the inclusion of oxidation in the diffusion model is user-specified. Whether this process be present or not, the initial node placement is obtained by equidistributing the modulus of the second derivative of the transformed initial distribution raised to the power of two-fifths. Carey and Hung [27] have proved this to be optimal for piecewise linear functions.

Consider now the case when oxidation is present. We assume that initially the motion of the interface dominates the diffusion effect in the silicon region. In order to determine an approximate initial profile close to the interface, whose motion is to be taken into account, (2.3) is modified to

$$0 = D_i \frac{\partial^2 c_s}{\partial x^2} + \dot{s}(0) \frac{\partial c_s}{\partial x} \quad . \tag{3.6}$$

A solution of (3.6) is

$$c_s = \exp\left\{ - \frac{\dot{s}(0)}{D_i} x \right\} \quad , \tag{3.7}$$

which can be expressed in non-dimensional variables as

$$C_s = \exp\left\{ - \frac{S_0 \, S'(0)}{L} X \right\} / n_i \quad . \tag{3.8}$$

We now perform a second equidistribution (in an identical manner as before) of a specified number of nodes (namely 2), to (3.8) between the interface and its nearest silicon node from the previous equidistribution. Since the transformation (3.1) does not significantly affect the profile (3.8), the above resulting arrangement of nodes is used as the silicon mesh on which the initial Gaussian is to be represented.

3.1.4 Treatment of Inconsistent Initial Data

In this section we describe a procedure to overcome the numerical problems caused by the initial inconsistency of the Gaussian (2.15)(a) with the interface condition (2.19)(a).

We begin by sampling point values of the transformed initial data (2.15)(a) at the nodal positions (the determination of which has been described in the previous section). The interface condition (3.4) is discretised using

$$\frac{1}{\delta_2}\,\frac{C_{s,I}\,D_S(C_{s,I})}{C_{s,I}+1}\left\{\frac{\Phi_{s,J}-\Phi_{s,I}}{\Delta X_1}\right\} + S'(0)\,[1-\gamma/m]\,C_{s,I} = 0 \quad , \tag{3.9}$$

where the additional I and J suffices respectively denote values at the interface and its adjacent node, and ΔX_1 represents the length of the first silicon element. We then rearrange (3.9) and apply a Picard iteration of the form

$$\left.\begin{aligned} \Phi_{s,I}^{(k)} &= C_{s,I}^{(k)} + \ln\{C_{s,I}^{(k)}\} \\ \Phi_{s,I}^{(k+1)} &= \Phi_{s,J} + \Delta X_1 \delta_2\,(1-\gamma/m)\,S'(0)\,\frac{C_{s,I}^{(k)}+1}{D_S(C_{s,I}^{(k)})} \end{aligned}\right\} \quad K \geq 0 \ . \tag{3.10}$$

Note that $\Phi_{s,J}$ remains unchanged, and that the first iterate is supplied by the initial data sampling.

In practice only one iteration is required to satisfy the convergence criterion.

3.1.5 Determination of Interface Dopant Concentration

We determine the interface dopant concentration in the oxidising silicon at each time-step by applying an iterative technique to (3.4). The process can be summarised as follows:-

(i) Estimate the interface nodal value velocity.

(ii) Set up the full MFE system, overwrite it with the interface nodal value velocity estimate, and then solve it for all nodal position and value velocities.

(iii) Temporarily update the interface nodal position and value, and those of the adjacent silicon node.

(iv) Determine whether or not the discretised form of the moving interface condition at the next time level is sufficiently satisfied; if not, then adjust the interface nodal value velocity and return to (ii).

(v) Repeat steps (ii)-(iv), but with a reduced system for the nodal value velocities only.

We now present a more detailed description of the above algorithm. The velocity at the previous time-step (except initially, when a value of zero is assumed) provides a reasonable first guess in (i). The conjugate gradient method ([24]) of section 3.1.1 is implemented in stage (ii), and in practice requires two or three iterations for inversion ([25]). Temporary updating of the nodal positions and values (denoted by the twiddle symbol) is respectively provided for by

$$\left.\begin{aligned} \tilde{X}^{(k)}_{s,M} &= X_{s,M} + \Delta T^{(k)} \dot{X}^{(k)}_{s,M} \\ \tilde{\Phi}^{(k)}_{s,M} &= \Phi_{s,M} + \Delta T^{(k)} \dot{\Phi}^{(k)}_{s,M} \end{aligned}\right\} \quad M = I,J \quad , \quad k \geq 0 \ , \tag{3.11}$$

where $\Delta T^{(k)}$ is the time increment at the k^{th} iteration step. $\Delta T^{(k)}$ is chosen to allow potentially overtaking nodes to move no further than half the collision distance, and to restrict the relative changes of the silicon element slopes, interface dopant concentration and values of the diffusion function at the nodes by 10%, 10% and 20% respectively.

Consider now stage (iv) of the procedure. We discretise the moving interface condition (3.4) in an identical way to that described in 3.1.4, and let

$$F(\tilde{\Phi}_{s,I}) = \frac{1}{\delta_2} \frac{\tilde{C}_{s,I} D_S(\tilde{C}_{s,I})}{\tilde{C}_{s,I} + 1} \left\{ \frac{\tilde{\Phi}_{s,J} - \tilde{\Phi}_{s,I}}{\Delta \tilde{X}_1} \right\} + \tilde{S}'(\tilde{T})[1-\gamma/m]\tilde{C}_{s,I} \ , \tag{3.12}$$

with $\tilde{C}_{s,I}$ obtained from $\tilde{\Phi}_{s,I}$ via a Newton inversion of (3.1). The criterion for convergence of F to zero is taken as

$$|F(\tilde{\Phi}_{s,I})| < \epsilon_1 \ , \tag{3.13}$$

which, if not satisfied, necessitates the evaluation of

$$F_\Phi(\tilde{\Phi}_{s,I}) \equiv \frac{\partial F}{\partial \tilde{\Phi}_{s,I}}(\tilde{\Phi}_{s,I}) \ . \tag{3.14}$$

The interface velocity potential value at the next time level is now predicted, using the Newton formula, as

$$\tilde{\Phi}^{(k)}_{s,I} = \tilde{\Phi}^{(k-1)}_{s,I} - \frac{F\left(\tilde{\Phi}^{(k-1)}_{s,I}\right)}{F_{\Phi}\left(\tilde{\Phi}^{(k-1)}_{s,I}\right)}, \quad k \geq 1 \quad . \tag{3.15}$$

Our new estimate of the nodal value velocity is taken as

$$\dot{\Phi}^{(k)}_{s,I} = \frac{\tilde{\Phi}^{(k)}_{s,I} - \Phi_{s,I}}{\Delta T^{(k)}} \quad , \quad k \geq 1 \; . \tag{3.16}$$

The full MFE system in (ii) is now overwritten using (3.16), and steps (ii) to (iv) are repeated until convergence is obtained.

Step (v) is introduced into the algorithm in order to save on computational time, since in one dimension we can employ an efficient tridiagonal solver for the symmetric nodal value velocity system. The nodal position velocities and time increment, which remain unaltered throughout the second iteration stage, are supplied by the last step of the first iteration procedure, as is the first estimate of the interface nodal value velocity. As in the first stage, we discretise (3.4) using (3.12) and investigate convergence via

$$|F(\tilde{\Phi}_{s,I})| < \epsilon_2 \quad . \tag{3.17}$$

If (3.17) is not satisfied, then evaluation of (3.14), (3,15) and (3.16) must be performed together with a further iteration.

The convergence tolerances in (3.13) and (3.17) are given by

$$\epsilon_1 = \tfrac{1}{2} \times 10^{-1} \quad , \quad \epsilon_2 = \tfrac{1}{2} \times 10^{-3} \quad . \tag{3.18}$$

In practice, stages one and two of the iteration process are performed only about one and two times respectively.

3.2 Determination of Oxide Dopant Concentration Profiles

In section 2.2 we obtained a purely hyperbolic first order p.d.e., (2.17), governing the behaviour of dopant in the oxide. This implies that any profile in this region maintains its original shape and is propagated at a velocity

$$-\delta_2[\gamma-1]\, S'(T) \ .$$

Any oxide initially present contains dopant whose concentration is given by (2.15)(b). Subsequent interface concentrations can be acquired from (2.19)(b).

In practice, we adopt the following procedure in order to obtain the required profiles. The initial interface dopant concentration is obtained from (2.19)(b) and stored, as is the length of the region if oxide is present at the outset. At subsequent times, the interface concentration is evaluated (from (2.19)(b)), and if significantly different from the previously-recorded one, both it and the present length of the oxide region are stored. Each required profile is then displayed according to the following:-

(i) Determine the location of the external oxide boundary and the interface dopant concentration.

(ii) Plot all recorded concentrations at their corresponding lengths from the boundary. Plot also the concentration in (i) at the interface position.

(iii) Connect all points in (ii) using straight-line segments.

In this way we obtain adquate representations of dopant profiles in the oxide region, without requiring large amounts of computation.

4. RESULTS

We now present results of the simplified problem, in which we solve for the transformed variable of the concentration.

4.1 Physical Data

The initial Gaussian implant is defined by

$$N = 10^{16}\,cm^{-2} \quad , \quad \sigma = 0.05\mu m \quad , \quad R = 0.25\mu m \quad , \tag{4.1}$$

and the following physical parameters are used:

$$\left.\begin{array}{lll} n_i = 2.80 \times 10^{18}\,cm^{-3} & , & D_i = 2.64 \times 10^{-9}\,\mu m^2 s^{-1} \\ \alpha = 1.50 & , & \beta = 100.0 \\ \gamma = 2.27 & , & m = 10.0 \end{array}\right\} . \tag{4.2}$$

When oxidation is not considered the domain is given by

$$s_l = 0.0\mu m \quad , \quad s_r = 1.0\mu m \quad , \tag{4.3)(a}$$

but when this process is included, an oxide thickness of $10\mathring{A}$ at the outset gives rise to the initial region:

$$s_l(0) = -0.001\mu m \quad , \quad s(0) = 0.0\mu m \quad , \quad s_r = 1.0\mu m \quad . \tag{4.3)(b}$$

4.2 Presentation and Analysis of Graphical Output

Figures 1-6 show logarithmic plots (in order to emphasize the essential features) of the concentration variable, C (in cm^{-2}), against the depth

(in μm). In all graphs the final output time is 10,000 seconds and 23 internal nodes are used. Total and clustered concentrations are respectively represented by full and broken lines. In figures 1, 3 and 5, where the concentration axis denotes the fixed external silicon boundary, we see the initial profile and its resulting shape. In figures 2, 4 and 6 the vertical axis, however, represents the final left-hand position of the oxide region, in which only the final configuration is displayed.

Consider, firstly the silicon region. Clearly visible in all figures is the effect of the diffusion, which increases with temperature (as does the distance travelled by the front and the magnitude of its gradient). We see that the clustered components behave like the total concentration for lower values, but can be significantly different for higher ones. The motion of the interface causes the dopant concentrations in figures 2, 4 and 6 to be slightly higher than their corresponding ones in 1, 3 and 5. This process also produces additional movement of the right-hand front.

Owing to the nature of the interface condition (2.19)(b), the oxide dopant concentration profiles are merely scaled records of the dopant behaviour at the interface, as driven by the silicon. In figures 2, 4 and 6 we observe that more oxide is grown at higher temperatures than lower ones, and that the profiles within are vastly different. The Gaussian peak is still far from the interface in figure 2, whereas it has almost reached the interface in 4. Impact has, however, already taken place in figure 6, where the

concentration profile is similar to that of 4, but contains an additional shallow piece near the interface.

Our results compare favourably with experiment. Because we do not consider enhanced diffusion due to point defect generation at the interface, however, we are unable to compare them with those given in [12].

4.3 Comparison of C.P.U. Times Used

Table 1 shows the C.P.U. time (in seconds) used on a Norsk Data mini computer when simulating both with and without oxidation at various temperatures.

	TEMPERATURE (°C)					
	850		900		950	
	NO OXID.	OXID.	NO OXID.	OXID.	NO OXID.	OXID.
C.P.U. TIME USED (secs.)	14.5	25.6	33.1	73.2	68.6	217.7

Table 1.

The above figures indicate a very efficient solution method for the simplified oxidation-diffusion problem. We see that simulations without oxidation at additional 50°C intervals cause the computer time used to be approximately doubled, whereas with the inclusion of oxidation these values increase by a factor of about three.

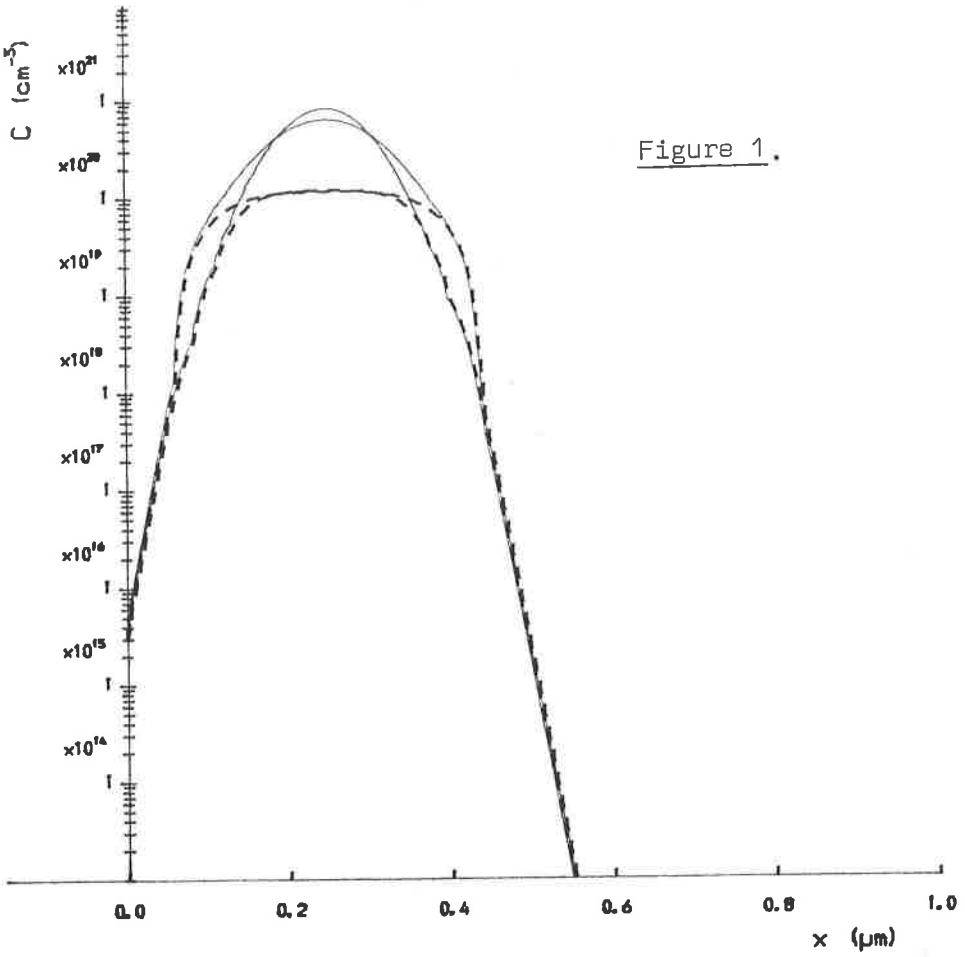

Figure 1.

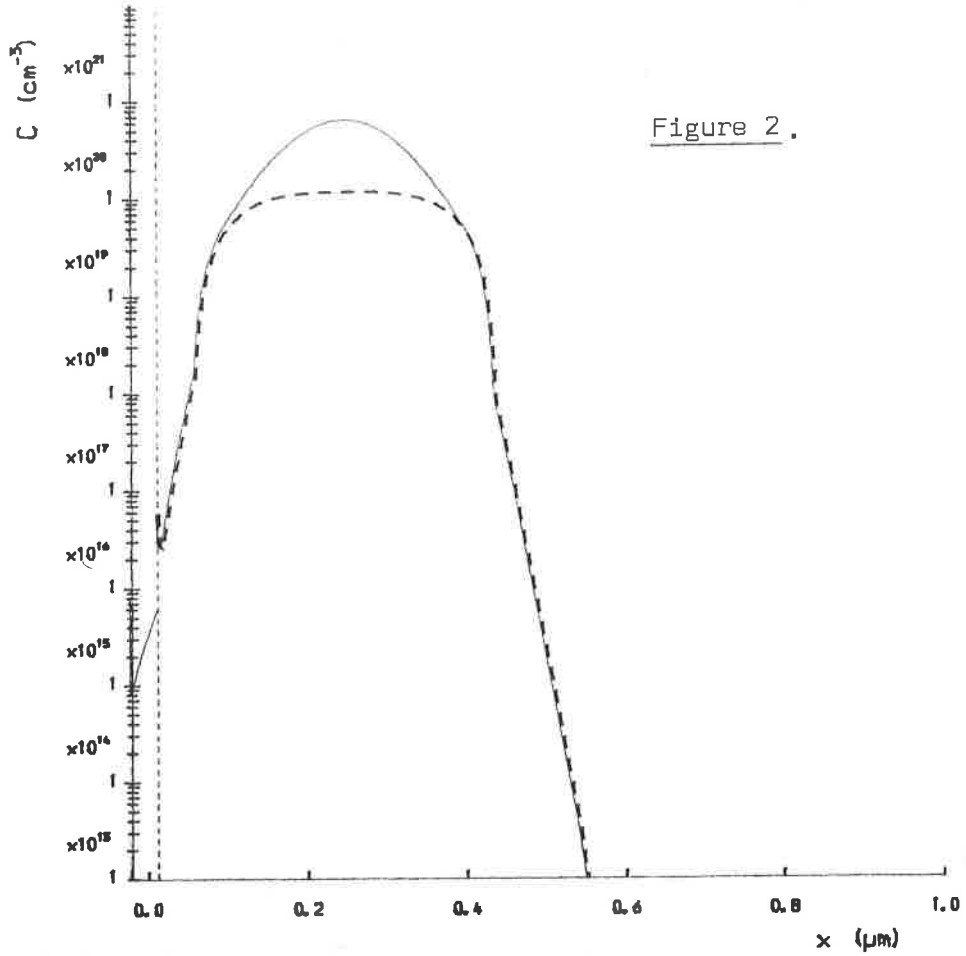

Figure 2.

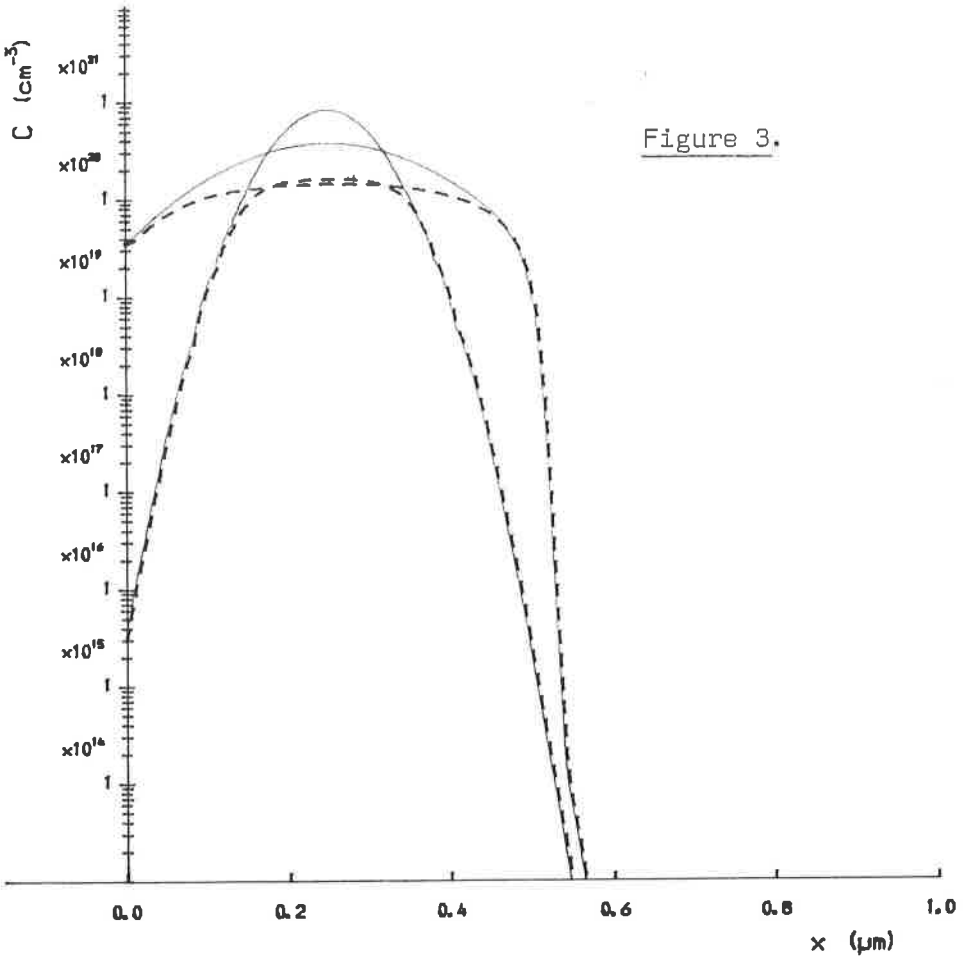

Figure 3.

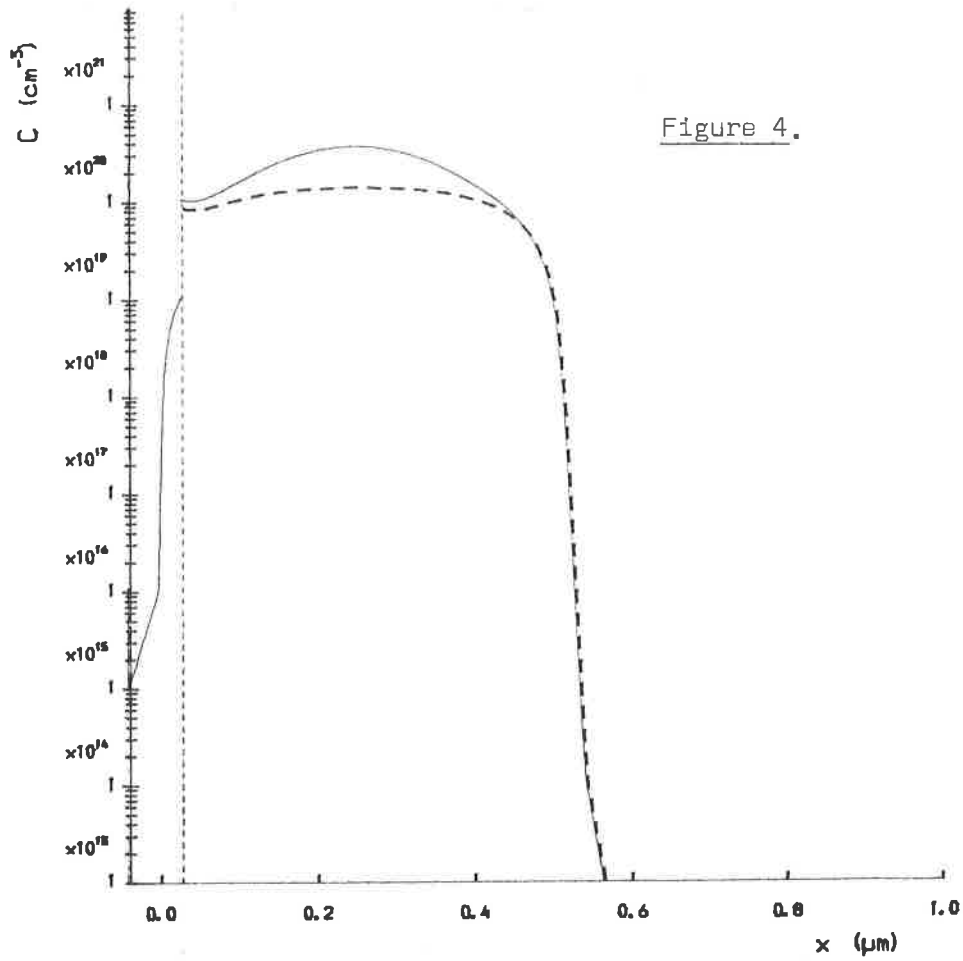

Figure 4.

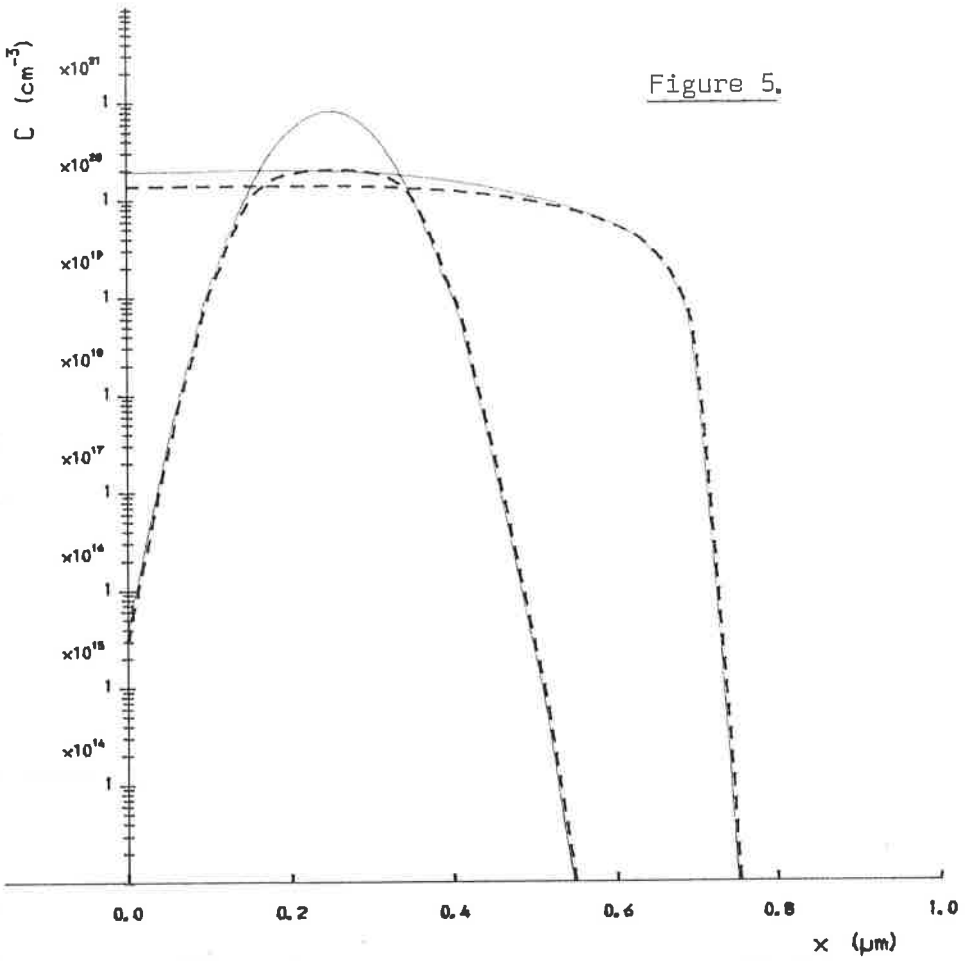

Figure 5.

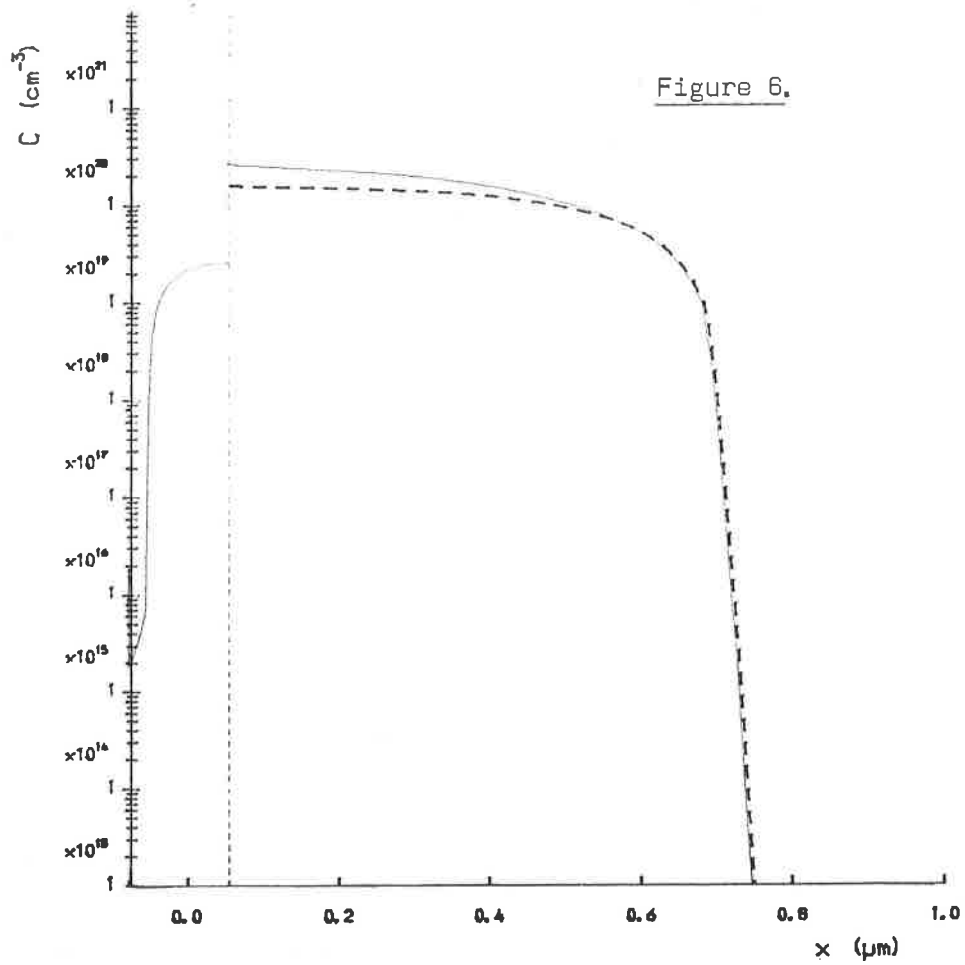

Figure 6.

5. CONCLUSIONS

In this paper we have presented a one-dimensional model governing the redistribution of dopant during the thermal oxidation of silicon. We have described how a non-dimensionalisation of the original problem leads to a much simpler partially decoupled one, in which oxide dopant profiles can be obtained once the silicon sub-problem has been solved at the desired time. The moving finite element method has been applied to a transformed variable in the silicon region, and has efficiently produced satisfactory results.

We hope next to extend the ideas of this paper to a two-dimensional oxidation-diffusion model.

ACKNOWLEDGEMENTS

The authors would like to thank Drs. M.J. Baines and P.K. Sweby, both of the Mathematics Department at Reading University, for their assistance throughout the duration of this work.

The support of the SERC is also acknowledged by both authors, the first being in receipt of a CASE award in association with GEC and the second being a SERC Research Fellow.

This work contributes towards the Alvey Directorate research program VLSI project 066.

REFERENCES

[1] DEAL, B.E. and GROVE, A.S., "General Relationship for the Thermal Oxidation of Silicon", J. Appl. Phys., vol. 36, no. 12, pp. 3770-3778, 1965.

[2] MASSOUD, H.Z., PLUMMER, J.D. and IRENE, E.A., "Thermal Oxidation of Silicon in Dry Oxygen - Accurate Determination of the Kinetic Rate Constants", J. Electrochem. Soc. vol. 132, no. 7, pp. 1745-1753, 1985.

[3] KING, J.R., "Some Analytical Results for the Local Oxidation of Silicon", in Proc. NASECODE IV Conf. (Ed. Miller, J.J.H.), Trinity College, Dublin, Ireland, pp. 339-345, 1985.

[4] STETTLER, J.C., WEISS, P., MORET, J.M. and LUGINBUEHL, H., "Simulation of Local Oxidation of Silicon for Plane and Non-Plane Surfaces", in Proc. NASECODE IV Conf. (Ed. Miller, J.J.H.), Trinity College, Dublin, Ireland, pp. 513-518, 1985.

[5] CHORIN, A.J., "A Numerical Method for Solving Incompressible Viscous Flow Problems", J. Comp. Phys., vol. 2, no. 1, pp. 12-26, 1967.

[6] CHIN, D., OH, S.-Y., HU, S.M., DUTTON, R.W. and MOLL, J.L., "Two-Dimensional Oxidation", IEEE Trans. Electron Devices, vol. ED-30, no. 7, pp. 744-749, 1983.

[7] CHIN, D., OH, S.-Y. and DUTTON, R.W., "A General Solution Method for Two-Dimensional Nonplanar Oxidation", IEEE Trans. Electron Devices, vol. ED-30, no. 9, pp. 993-998, 1983.

[8] BORUCKI, L. and SLINKMAN, J., "An Efficient Finite Element Algorithm for Modeling Two-Dimensional Oxidation and Impurity Redistribution in Silicon", in Proc. NASECODE IV Conf. (Ed. Miller, J.J.H.), Trinity

College, Dublin, Ireland, pp. 226-233, 1985.

[9] MARTIN, S. and MATHIOT, D., "OLIMP: A New IC's Process 1D Simulator Using a Physical Model of Diffusion", in Proc. NASECODE IV Conf. (Ed. Miller, J.J.H.), Trinity College, Dublin, Ireland, pp.390-395, 1985.

[10] BAINES, M.J., PLEASE, C.P. and SWEBY, P.K., "Numerical Solution of Dopant Diffusion Equations", in "Simulation of Semiconductor Devices and Processes", vol. 2 (Ed. Board, K. and Owen, D.R.J.), Pineridge Press, Swansea, pp. 271-286, 1986.

[11] GERODOLLE, A., MARTIN, S. and MARROCCO, A., "Finite Element Method Applied to 2D MOS Process Simulation and Defect Diffusion: Program TITAN", in Proc. NASECODE IV Conf. (Ed. Miller, J.J.H.), Trinity College, Dublin, Ireland, pp. 287-292, 1985.

[12] BUDIL, M., JÜNGLING, W., GUERRERO, E., SELBERHERR, S. and PÖTZL, H., "Modeling of Point Defect Kinetics During Thermal Oxidation", in "Simulation of Semiconductor Devices and Processes", vol. 2 (Ed. Board, K. and Owen, D.R.J.), Pineridge Press, Swansea, pp. 384-397, 1986.

[13] PENUMALLI, B.R., "A Comprehensive Two-Dimensional VLSI Process Simulation Program, BICEPS", IEEE Trans. Electron Devices, vol. ED-30, no. 9, pp. 986-992, 1983.

[14] MALDONADO, C.D., CUSTODE, F.Z., LOUIE, S.A. and PANCHOLY, R., "Two-Dimensional Simulation of a 2-µm CMOS Process Using ROMANS II", IEEE Trans. Electron Devices, vol. ED-30, no. 11, pp. 1462-1469, 1983.

[15] TANIGUCHI, K., KASHIWAGI, M. and IWAI, H., "Two-Dimensional Computer Simulation Models for MOSLI Fabrication Processes", IEEE Trans. Electron Devices, vol. ED-28, no. 5, pp. 574-580, 1981.

[16] DESOUTTER, I., COLLARD, D. and DECARPIGNY, J.N., "Two Dimensional Simulation of Diffusion Under Oxidizing Ambients Using the Finite Element Method", in Proc. NASECODE IV Conf. (Ed. Miller, J.J.H.), Trinity College, Dublin, Ireland, pp. 267-271, 1985.

[17] KOLTAI, M. and TRUTZ, S., "Process Simulation on the IBM Personal Computer", in "Simulation of Semiconductor Devices and Processes", vol. 2 (Ed. Board, K. and Owen, D.R.J.), Pineridge Press, Swansea, pp. 580-593, 1986.

[18] BORUCKI, L., HANSEN, H.H. and VARAHRAMYAN, K., "FEDSS - A 2D Semiconductor Fabrication Process Simulator", IBM J. Res. Develop., vol. 29, no. 3, pp. 263-276, 1985.

[19] MILLER, K. and MILLER, R.N., "Moving Finite Elements, Part I", SIAM J. Numer. Anal., vol. 18, no. 6, pp. 1019-1032, 1981.

[20] MILLER, K., "Moving Finite Elements, Part II", SIAM J. Numer. Anal., vol. 18, no. 6, pp. 1033-1057, 1981.

[21] WATHEN, A.J. and BAINES, M.J., "On the Structure of the Moving Finite-element Equations", IMA J. Numer. Anal., vol. 5, pp. 161-182, 1983.

[22] FAIR, R.B., "Concentration Profiles of Disused Dopant in Silicon", in "Impurity Doping Processes in Silicon" (Ed. Wang, F.F.Y.), North-Holland, New York, pp. 315-442, 1981.

[23] JOHNSON, I.W., "The Moving Finite Element Method for the Viscous Burgers' Equation", Numer. Anal. Report 3/84, Dept. of Maths., Univ. of Reading.

[24] CONCUS, P., GOLUB, G.H. and O'LEARY, D.P., "A Generalized Conjugate Gradient Method for the Numerical Solution of Elliptic Partial Differential Equations", in "Sparse Matrix Computations" (Ed. Bunch, J.R. and Rose, D.J.), Academic Press, New York, pp. 309-332, 1976.

[25] WATHEN, A.J., "Attainable Eigenvalue Bounds for the Galerkin Mass Matrix" (submitted to IMA J. Numer. Anal.), School of Maths., Univ. of Bristol, 1986.

[26] PLEASE, C.P. and SWEBY, P.K., "A Transformation to Assist Numerical Solution of Diffusion Equations", Numer. Anal. Report 5/86, Dept. of Maths., Univ. of Reading.

[27] CAREY, G.F. and HUNG, T.D., "Grading Functions and Mesh Redistribution", SIAM J. Numer. Anal., vol. 22, no. 5, pp. 1028-1040, 1985.